

SINGULAR SOLUTIONS FOR SHALLOW SHELLS

W. FLÜGGE†

Department of Applied Mechanics, Stanford University, Stanford, California

and

R. E. ELLING‡

Departments of Civil Engineering and Engineering Mechanics, Clemson University,
Clemson, South Carolina

Abstract—Solutions are developed for non-axially symmetric shallow shells subjected to normal surface loading or thermal loading. The singular solutions which correspond to the concentrated normal load, the concentrated application of heat and the concentrated thermal gradient are identified by a consistent limiting process applied to the complete set of singular solutions. Numerical results are presented for the case of the normal concentrated load acting on shallow shells having negative, zero or positive Gaussian curvature.

The behavior of the shallow shells in the neighborhood of the applied concentrated load is seen to be similar to that of a disc subjected to the same load. The influence of the concentrated load is felt over a wider region in shells of negative Gaussian curvature compared to shells of positive Gaussian curvature. However, for the case of the concentrated load, the stress and deflection parameters of the shell do not change dramatically as the Gaussian curvature of the shell is varied from positive to negative values.

NOTATION

A_p, B_p, C_p, D_p	arbitrary constants of solution η
a	principal radius of curvature of shell at its vertex, lying in xz plane
$a_{m,n}, a_{\bar{m},n}, \bar{a}_{m,n}$	constants whose value depends on m, n
b	principal radius of curvature of shell at its vertex, lying in yz plane
c^2	$\kappa^2/2a^2$
D	membrane stiffness $Et/(1-\nu^2)$
E	Young's modulus
K	bending stiffness $Et^3/(1-\nu^2)$
q	distributed normal loading
R_n	function f_r , solution to differential equation
r	radial coordinate
$S_{s,t}$	parameter in solution for η
T	average temperature across section of shell
\bar{T}	temperature difference between two surfaces of shell
t	thickness of shell
u	displacement tangent to shell along meridian $\theta = \text{const.}$
v	displacement tangent to shell along circle $r = \text{const.}$
w	displacement normal to shell; positive w has principal component in positive z direction
x, y, z	rectangular Cartesian coordinates
α	$1 - a/b$
$\bar{\alpha}$	thermal coefficient of expansion

† Professor emeritus.

‡ Associate Professor.

γ	a/b
$\gamma_{r\theta}, \gamma_{xy}$	shear strain
δ	α/λ
$\varepsilon_x, \varepsilon_y, \varepsilon_r, \varepsilon_\theta$	normal strains
ζ	const., part of exponent of ξ
η	complex stress function
θ	angular coordinate
λ^4	$12(1-\nu^2)/(a/t)^2$
λ	$(1+a/b)/2$
μ	intensity of plane hot spot
$\bar{\mu}$	intensity of bending hot spot
ν	Poisson's ratio
ξ	dimensionless radial coordinate = $\sqrt{(t)}cr$
ρ	particular value of radial coordinate r at boundary of shell
Φ	stress function
Φ_m	parameter in solution η
∇^2	$\frac{\partial^2}{\partial x^2} + \frac{\partial^2}{\partial y^2}$
∇^4	$\nabla^2 \times \nabla^2$
∇^2	$\frac{d^2}{d\xi^2} + \frac{1}{\xi} \frac{d}{d\xi} - \frac{n^2}{\xi^2}$

INTRODUCTION

THE bending theory of thin elastic shells involves a set of equations of sufficient complexity so that there is no simple general solution. However, if one restricts the slope of the shell to small values, thereby obtaining a "shallow shell", great simplifications are possible in the general shell equations, and these simplified equations open up an avenue through which the behavior of a more general shell may be explored. Of particular interest among the solutions to the shallow shell equations are those singular solutions which represent concentrated forces and concentrated areas of heating. Since almost any shell has a small slope within a restricted region, the solutions for concentrated loads applied to shallow shells can also be considered to be the solutions, in a localized region, for a more general shell having the same geometry around the point of loading as does the shallow shell.

Many investigators have made significant contributions to the development of the shallow shell theory, and in particular, to the identification of the singular solutions which represent concentrated loading or heating. Chernyshev [1] has proven that the dominant part of the singular solution corresponding to the application of a concentrated force or moment on a general shell is the same as that for the same loading applied to a flat plate. Among those who have developed and identified singular solutions for special geometrical forms are Young [12] who developed a wide range of solutions for a spherical shell; Flügge and Conrad [5] who presented singular solutions for thermal "hot spots" applied to cylindrical shells; Sanders and Simmonds [8], who obtained the solution for a concentrated normal force applied to a shallow cylindrical shell; and Forsberg and Flügge [3], who investigated the solution for point loads applied to elliptical shells. A recent paper by Sanders [9] presents a unified treatment of the shallow shell equations with solutions in the form of Fourier transforms.

The objective of this paper is to present the solutions for a concentrated normal force and for concentrated heating applied to nonaxisymmetric shallow shells, and in particular,

to show the influence of shell geometry on the nature of the singular solutions throughout the shell.

BASIC EQUATIONS

The basic partial differential equations which govern the behavior of shallow shells can be reduced to a pair of equations for a stress function Φ and the normal displacement w . The equations are [4]:

$$Q\Phi - K\nabla^4 w = -q + \frac{K(1+\nu)}{t} \bar{\alpha} \nabla^2 \bar{T} \quad (1)$$

$$\nabla^4 \Phi + D(1-\nu^2)Qw = -D(1-\nu^2)\bar{\alpha} \nabla^2 T$$

where

$$D = \frac{Et}{1-\nu^2}, \quad \text{the membrane stiffness}$$

$$K = \frac{Et^3}{12(1-\nu^2)}, \quad \text{the bending stiffness}$$

and

$$\nabla^2 = \frac{\partial^2}{\partial x^2} + \frac{\partial^2}{\partial y^2}, \quad \text{a differential operator}$$

$$\nabla^4 = \nabla^2 \times \nabla^2, \quad \text{a differential operator}$$

$$Q = z_{,xx} \frac{\partial^2}{\partial y^2} + 2z_{,xy} \frac{\partial^2}{\partial x \partial y} + z_{,yy} \frac{\partial^2}{\partial x^2}, \quad \text{a differential operator}$$

q = distributed load normal to shell surface;

$\bar{\alpha}$ = coefficient of thermal expansion;

T = average temperature over a section of shell;

\bar{T} = temperature difference between inner and outer shell surface.

Figure 1 shows the basic coordinate system used in these expressions.

Although the differential equations do not place a restriction on the shell geometry, apart from that of the shallow shell assumptions, we will restrict our investigation to paraboloids expressed by:

$$z = \frac{1}{2a}x^2 - \frac{1}{2b}y^2.$$

Here a and b are the two principal radii of curvature of the shell at its apex, and if both are positive, the equation describes a shell of negative curvature—a hyperbolic paraboloid. The cylinder is described by the equation when $b \rightarrow \infty$, and a sphere is described when $b = -a$.

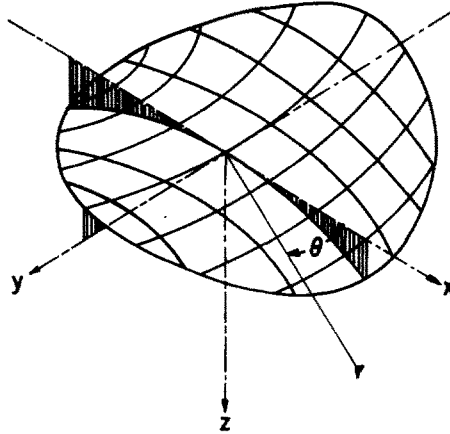


FIG. 1. Coordinate system for shallow shell.

We seek first to obtain solutions for the homogeneous equations, and therefore set $q = T = \bar{T} = 0$. The two 4th-order equations (1) may then be linearly combined in two different ways [3], thereby producing a single 4th-order equation :

$$\nabla^4 \eta + \frac{i\kappa^2}{a} Q\eta = 0$$

where

$$\frac{\kappa^2}{a} = \left[\frac{D(1-\nu^2)}{K} \right]^{\frac{1}{2}} \tag{2}$$

and η can have either of the definitions :

$$\eta = \Phi - iK \frac{\kappa^2}{a} w \tag{3a}$$

or

$$\eta = K \frac{\kappa^2}{a} w + i\Phi. \tag{3b}$$

The solution to the single 4th-order equation (2) thus produces the full set of solutions to the pair of equations (1) when both definitions of η in equation (3) are used in turn to define the dependent variable.

Coordinate system

Although the basic differential equations were developed in Cartesian coordinates, we are here faced with the necessity of finding a coordinate system which will permit a separation of variables and will also permit a straightforward method of producing and identifying singular solutions to these equations. The polar coordinate system r, θ will permit meeting these objectives and will be used in the remainder of this work.

When the differential equation (2) is transformed to polar coordinates, the result is :

$$\begin{aligned} \nabla^4 \eta + i \frac{\kappa^2}{2a^2} \left[\alpha \nabla^2 \eta + 2\lambda \cos 2\theta \left(-\frac{\partial^2}{\partial r^2} + \frac{1}{r} \frac{\partial}{\partial r} + \frac{1}{r^2} \frac{\partial^2}{\partial \theta^2} \right) \eta \right. \\ \left. + 4\lambda \sin 2\theta \left(\frac{1}{r} \frac{\partial^2}{\partial \theta \partial r} - \frac{1}{r^2} \frac{\partial}{\partial \theta} \right) \eta \right] = 0 \end{aligned} \tag{4}$$

where

$$\nabla^2 = \frac{\partial^2}{\partial r^2} + \frac{1}{r} \frac{\partial}{\partial r} + \frac{1}{r^2} \frac{\partial^2}{\partial \theta^2}, \quad \lambda = \frac{1}{2}(1 + a/b) \quad \text{and} \quad \alpha = 1 - a/b.$$

METHOD OF SOLUTION

As a first step in the solution of equation (4), we separate variables r, θ by postulating a solution in the form of a harmonic series:

$$\eta = \sum_{n=0, \pm 1, \pm 2, \dots}^{\pm \infty} R_n(r) \cos(n\theta). \quad (5)$$

Similar solutions may also be written in terms of sin series; however, to simplify the discussion in this work, we will restrict our attention to the cos series. The use of both positive and negative integer values of n leads to some simplifications in the subsequent development of the differential equations. When equation (5) is substituted in equation (4), and we shift indices to obtain a common factor $\cos n\theta$, the result is:

$$\begin{aligned} & \sum_{n=0, \pm 1, \pm 2, \dots}^{\pm \infty} \left\{ \left(\frac{d^2}{dr^2} + \frac{1}{r} \frac{d}{dr} - \frac{n^2}{r^2} \right)^2 R_n \right. \\ & + \frac{ik^2}{2a^2} \left[\alpha \left(\frac{d^2}{dr^2} + \frac{1}{r} \frac{d}{dr} - \frac{n^2}{r^2} \right) R_n - \lambda \left(\frac{d^2}{dr^2} - \frac{(2n-3)}{r} \frac{d}{dr} + \frac{n(n-2)}{r^2} \right) R_{n-2} \right. \\ & \left. \left. - \lambda \left(\frac{d^2}{dr^2} + \frac{(2n+3)}{r} \frac{d}{dr} + \frac{n(n+2)}{r^2} \right) R_{n+2} \right] \right\} \cos n\theta = 0. \quad (6) \end{aligned}$$

Equation (6) may be satisfied if we require that the coefficient of $\cos n\theta$ vanish identically for each positive and negative value of n . Thus, we obtain:

$$\begin{aligned} & \left(\frac{d^2}{dr^2} + \frac{1}{r} \frac{d}{dr} - \frac{n^2}{r^2} \right)^2 R_n + \frac{ik^2}{2a^2} \left[\alpha \left(\frac{d^2}{dr^2} + \frac{1}{r} \frac{d}{dr} - \frac{n^2}{r^2} \right) R_n \right. \\ & - \lambda \left(\frac{d^2}{dr^2} - \frac{(2n-3)}{r} \frac{d}{dr} + \frac{n(n-2)}{r^2} \right) R_{n-2} \\ & \left. - \lambda \left(\frac{d^2}{dr^2} + \frac{(2n+3)}{r} \frac{d}{dr} + \frac{n(n+2)}{r^2} \right) R_{n+2} \right] = 0, \quad n = 0, \pm 1, \pm 2, \dots \pm \infty. \quad (7) \end{aligned}$$

Equation (7) produces solutions R_n for both positive and negative n ; however, the only significant solutions are expressed as:

$$\bar{R}_n = R_n + R_{-n}. \quad (8)$$

Equation (7) represents a set of ordinary differential equations, coupled together in adjoining values of n . Since the differential equation for R_n is coupled only to those for

R_{n+2} and R_{n-2} , the equations for even integer values of n form a separate set, independent of those for odd integer values of n . Thus, solutions for even and odd values of n must be developed independently; however, the technique used in developing the two sets of solutions is identical.

Equation (7) may be written in slightly simpler form by the introduction of some new notation. We let:

$$\begin{aligned} \zeta &= \left[\frac{i\kappa^2}{2a^2} \right]^{\frac{1}{2}} r = [i]^{\frac{1}{2}} cr; \\ c^2 &= \frac{\kappa^2}{2a^2} = \frac{[3(1-\nu^2)]^{\frac{1}{2}}}{at} \\ \nabla_n^2 &= \frac{d^2}{d\xi^2} + \frac{1}{\xi} \frac{d}{d\xi} - \frac{\eta^2}{\xi^2}. \end{aligned}$$

With the use of this notation, equation (7) becomes:

$$\begin{aligned} &[\nabla_n^4 + \alpha \nabla_n^2] R_n - \lambda \left[\frac{d^2}{d\xi^2} - \frac{(2n-3)}{\xi} \frac{d}{d\xi} + \frac{n(n-2)}{\xi^2} \right] R_{n-2} \\ &- \lambda \left[\frac{d^2}{d\xi^2} + \frac{(2n+3)}{\xi} \frac{d}{d\xi} + \frac{n(n+2)}{\xi^2} \right] R_{n+2} = 0, \quad n = 0, \pm 1, \pm 2, \dots \pm \infty. \end{aligned} \tag{9}$$

Equation (9) is the basic form of the differential equation which will be used in the subsequent development of the solutions.

Solution of infinite set of ordinary differential equations

The solution of the infinite set of ordinary differential equations is developed systematically by postulating the solution in the form of an infinite power series, i.e. by the Frobenius method [6]. The form of the postulated solution which leads to a general solution may be shown to be [2]:

$$R_n = \log \xi \sum_{m=0,1,2,\dots}^{\infty} a_{m,n} \xi^{m+\zeta} + \sum_{m=0,1,2,\dots}^{\infty} b_{m,n} \xi^{m+\zeta} \tag{10}$$

where $a_{m,n}$, $b_{m,n}$ and ζ are as yet undetermined quantities. Substitution of equation (10) in (9) produces results from which the following recurrence relationships between the constants $a_{m,n}$ and $b_{m,n}$ may be obtained:

$$\begin{aligned} \bar{a}_{\bar{m},n} &= -\delta \bar{a}_{\bar{m}-2,n} + \bar{a}_{\bar{m}-2,n-2} + \bar{a}_{\bar{m}-2,n+2}, & \bar{m} > |n| + 2 \\ \bar{b}_{\bar{m},n} &= -\delta \bar{b}_{\bar{m}-2,n} + \bar{b}_{\bar{m}-2,n+2} + \bar{b}_{\bar{m}-2,n+2}, & -|n| + 2 < \bar{m} < |n| \end{aligned} \tag{11}$$

and

$$\begin{aligned} \bar{b}_{\bar{m},n} &= \frac{2\delta \bar{m}}{(\bar{m}+n)(\bar{m}-n)} \bar{a}_{\bar{m}-2,n} - \frac{2(\bar{m}+n-1)}{(\bar{m}+n)(\bar{m}+n-2)} \bar{a}_{\bar{m}-2,n-2} - \frac{2(\bar{m}-n-1)}{(\bar{m}-n)(\bar{m}-n-2)} \bar{a}_{\bar{m}-2,n+2} \\ &- \delta \bar{b}_{\bar{m}-2,n} + \bar{b}_{\bar{m}-2,n+2} + \bar{b}_{\bar{m}-2,n+2}, \quad \bar{m} > |n| + 2. \end{aligned}$$

In equations (11) we have introduced the following notation: $\delta = \alpha/\lambda$, $\bar{m} = m + \zeta$, where \bar{m} is an integer ranging from $-\infty$ to ∞ ,

$$a_{\bar{m},n} = \left[\frac{\lambda^{\bar{m}/2}}{2^{\bar{m}} \left(\frac{\bar{m}+n}{2}\right)! \left(\frac{\bar{m}-n}{2}\right)!} \right] \bar{a}_{\bar{m},n}, \quad \bar{m} > |n| + 2$$

$$b_{\bar{m},n} = \left[\frac{\lambda^{\bar{m}/2} \left(\frac{|n| - \bar{m} - 2}{2}\right)!}{2^{\bar{m}} \left(\frac{|n| + \bar{m}}{2}\right)!} \right] \bar{b}_{\bar{m},n}, \quad -|n| + 2 < \bar{m} < |n|$$

and

$$b_{\bar{m},n} = \left[\frac{\lambda^{\bar{m}/2}}{2^{\bar{m}} \left(\frac{\bar{m}+n}{2}\right)! \left(\frac{\bar{m}-n}{2}\right)!} \right] \bar{b}_{\bar{m},n}, \quad \bar{m} > |n| + 2.$$

Recurrence equations (11) indicate that each $\bar{a}_{\bar{m},n}$ or $\bar{b}_{\bar{m},n}$ depends for its value on either 3 or 6 other constants having a lesser value of the index \bar{m} . However, it may be shown that arbitrary values may be assigned to certain constants without violating equation (10); therefore, the application of recurrence equations (11) begins from these arbitrary constants. Four such arbitrary constants exist for each value of n and these are shown schematically in Fig. 2. As can be seen from Fig. 2 the arbitrary constants $\bar{b}_{\bar{m},n}$ are located along diagonals $\bar{m} = \pm n$ and $\bar{m} = \pm n + 2$. In addition, four specific $\bar{a}_{\bar{m},n}$ may be assigned arbitrary values; these are $a_{0,0}$, $a_{0,2}$, $a_{-1,1}$ and $a_{1,1}$. The arbitrary constants $\bar{b}_{\bar{m},n}$ on the diagonals $\bar{m} = |n|$ and $\bar{m} = |n| + 2$ produce singular solutions, while the arbitrary constants on the diagonals $\bar{m} = -|n|$ and $\bar{m} = -|n| + 2$ produce singular solutions. It may also be shown that all $\bar{b}_{\bar{m},n}$ in the region to the left of the diagonals $\bar{m} = -|n|$, and all $\bar{a}_{\bar{m},n}$ in the region to the left of the diagonals $\bar{m} = |n|$, are identically zero.

The recurrence equations (11) may be applied repeatedly, starting from an arbitrary constant, to produce a numerical answer corresponding to a specific geometrical parameter a/b . However, in order to gain greater insight into the nature of the general solution, and in order to develop a method of identifying singularities, we now use the recurrence equations to develop an explicit expression for a general solution. The method used to accomplish this end is essentially trial and inspection. A single $\bar{a}_{\bar{m},n}$ or $\bar{b}_{\bar{m},n}$ to which an arbitrary value may be assigned, is given the value unity, and all other arbitrary constants are set equal to zero. The appropriate recurrence relationship is used repeatedly to establish the propagation pattern of the solution, and an attempt is then made to express the propagation pattern explicitly.

The development of the recurrence equation into an explicit expression for a solution is demonstrated for the cylinder ($b \rightarrow \infty$) whose geometry leads to somewhat simpler results than the case of general a/b . For the cylinder, the α , λ and δ assume the following values:

$$\alpha = 1, \quad \lambda = \frac{1}{2}, \quad \delta = 2.$$

We assign the value unity to an arbitrary $\bar{b}_{\bar{m},n}$ on the diagonal $\bar{m} = n$ and apply recurrence equation (11) repeatedly. A typical pattern of numbers which results is shown in Fig. 3.

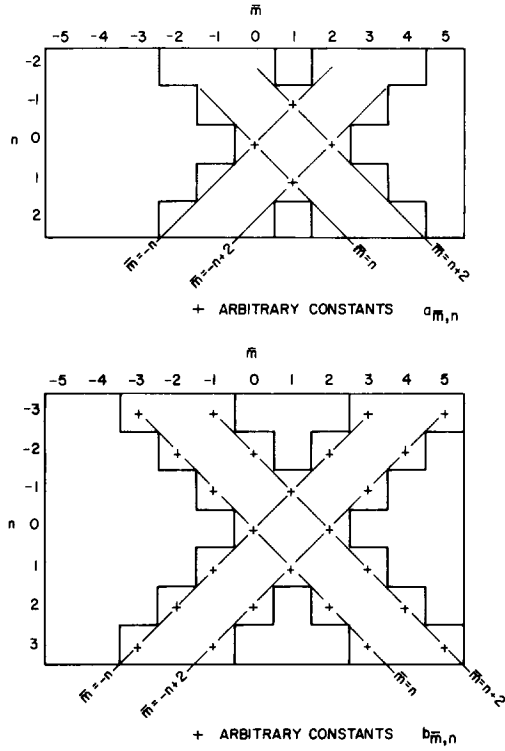


FIG. 2. (a), (b) Arbitrary constants $a_{\bar{m},n}$ and $b_{\bar{m},n}$.

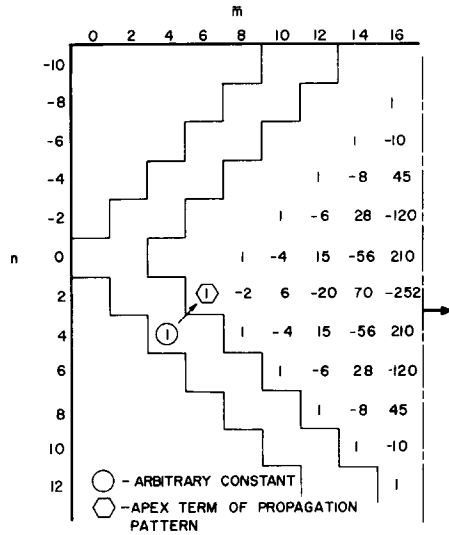


FIG. 3. Propagation pattern of $b_{\bar{m},n}$ for a cylinder solution.

The $\bar{b}_{\bar{m},n}$ shown for the illustration may be expressed explicitly by the relationship:

$$\bar{b}_{\bar{m},n} = \left(\frac{\bar{m} - p - 4}{\bar{m} - n - 4} \right) \frac{(-1)^{(\bar{m}+n)/2}}{2}, \quad \bar{m} > n + 2, p \neq 0$$

and

$$\bar{b}_{p,p} = 1, \quad \bar{m} = n = p \quad (12)$$

where the subscript p describes the specific value of n associated with the $\bar{b}_{\bar{m},n}$ which is assigned the value unity. In equation (12) and in all subsequent expressions for the $\bar{a}_{\bar{m},n}$ and $\bar{b}_{\bar{m},n}$, we use the following definitions of binomial coefficients and factorials:

$$\binom{i}{j} = \frac{i!}{(i-j)!j!}, \quad i = 1, 2, \dots; \quad j = 1, 2, \dots < i$$

$$\binom{i}{0} = 1, \quad j = 0$$

$$\binom{0}{0} = 1, \quad i = j = 0$$

$$\binom{i}{j} = 0, \quad j < 0 \text{ or } j > i$$

$$0! = 1.$$

All regular and singular solutions for general a/b are developed in a manner similar to that shown for a portion of the cylinder solution; in each case, the resulting expression for the $\bar{a}_{\bar{m},n}$ and $\bar{b}_{\bar{m},n}$ involves binomial coefficients such as shown in equation (12). The solution η for a specific p is now written as:

$$\eta_p = \sum_{n=0, \pm 2}^{\pm \infty} \cos n\theta \left[\log \xi \sum_{\bar{m}=-p, -p+2, \dots}^{\infty} a_{\bar{m},n} \xi^{\bar{m}} + \sum_{\bar{m}=-p, -p+2, \dots}^{\infty} b_{\bar{m},n} \xi^{\bar{m}} \right] \quad p = 0, 2, 4. \quad (13)$$

There are four arbitrary constants associated with each p , and these are designated A_p , B_p , C_p and D_p . Equation (13) contains only the even harmonics; a similar expression exists which includes only the odd harmonics. The general solution for even harmonics, derived from the postulated form of solution, equation (10), and valid for arbitrary a/b , may then be written as follows:

For $p = 0$:

$$\begin{aligned}
 \eta_0 = & A_0 + B_0 \left\{ \lambda \left(\frac{\xi}{2} \right)^2 - \sum_{n=0, \pm 2, \dots}^{\pm \infty} \cos n\theta \sum_{\bar{m}=|n|+4, 6, \dots}^{\infty} N_{\bar{m}, n} \xi^{\bar{m}} \right. \\
 & \times \left. \sum_{h=0, 1, 2, \dots}^{\text{ent}(\bar{m}-n-4)/2} \binom{\frac{\bar{m}-4}{2}}{\frac{n}{2}+2h} \binom{\frac{n}{2}+2h}{h} \delta^{(\bar{m}-n)/2-1-2h} \right\} \\
 & + C_0 \left\{ -\log \xi + \sum_{n=0, \pm 2, \dots}^{\pm \infty} \cos n\theta \left[-2 \log \xi \sum_{\bar{m}=|n|+0, 2, \dots}^{\infty} N_{\bar{m}, n} \xi^{\bar{m}} \right. \right. \\
 & \times \left. \sum_{h=0, 1, 2, \dots}^{\text{ent}(\bar{m}-n)/2} \binom{\frac{\bar{m}-2}{2}}{\frac{n}{2}-1+2h} \binom{\frac{n}{2}-1+2h}{h} \delta^{(\bar{m}-n)/2-2h} \right. \\
 & \left. \left. + \sum_{\bar{m}=|n|+4, 6, \dots}^{\pm \infty} N_{\bar{m}, n} \xi^{\bar{m}} (\Psi_{\bar{m}, n})_1 \right] \right\} \\
 & + D_0 \left\{ \lambda \left(\frac{\xi}{2} \right)^2 \log \xi + \sum_{n=0, \pm 2, \dots}^{\pm \infty} \cos n\theta \left[-\log \xi \sum_{\bar{m}=|n|+2, 4, \dots}^{\infty} N_{\bar{m}, n} \xi^{\bar{m}} \right. \right. \\
 & \times 2 \sum_{h=0, 1, 2, \dots}^{\text{ent}(\bar{m}-n-2)/4} \binom{\frac{\bar{m}-4}{2}}{\frac{n}{2}-1+2h} \binom{\frac{n}{2}-1+2h}{h} \delta^{(\bar{m}-n)/2-1-2h} \\
 & + \log \xi \sum_{h=0, 1, \dots}^{\text{ent}(\bar{m}-n-4)/4} \binom{\frac{\bar{m}-4}{2}}{\frac{n}{2}+2h} \binom{\frac{n}{2}+2h}{h} \delta^{(\bar{m}-n)/2-1-2h} \\
 & \left. \left. + \sum_{\bar{m}=|n|+4, 6, \dots}^{\infty} N_{\bar{m}, n} \xi^{\bar{m}} (\Psi_{\bar{m}, n})_2 \right] \right\}. \tag{14}
 \end{aligned}$$

Solutions similar to those in equation (14), and slightly more complex in form, may be written for $p > 2$. In equation (14) we have introduced the following notation:

$$N_{\bar{m},n} = \frac{\lambda^{\bar{m}/2} (-1)^{(\bar{m}+n)/2}}{2^{\bar{m}} [(\bar{m}+n)/2]! [(\bar{m}-n)/2]!}$$

$$(\Psi_{\bar{m},n})_{1,2} = \sum_{s=4,6,\dots}^{\bar{m}} \sum_{t=0,\pm 2,\dots}^{\pm(s-4)} (S_{s,t})_{\frac{1}{2}} (-1)^{(\bar{m}+n-s-t)/2}$$

$$\times \sum_{h=0,1,2,\dots}^{\text{ent}((\bar{m}-n+t-s)/4)} \binom{\frac{\bar{m}-s}{2}}{\frac{n-t}{2}+2h} \binom{\frac{n-t}{2}+2h}{h} \delta^{(\bar{m}-n+t-s)/2-2h}$$

$$(S_{s,t})_{1,2} = \frac{2\delta s}{(s+t)(s-t)} (\bar{a}_{s-2,t})_{1,2} - \frac{2(s+t-1)}{(s+t)(s+t-2)} (\bar{a}_{s-2,t-2})_{1,2}$$

$$- \frac{2(s-t-1)}{(s-t)(s-t-2)} (\bar{a}_{s-2,t+2})_{1,2}$$

$\text{ent}(\) =$ nearest integer equal to or less than ().

The solution expressed by equation (19) can be shown [2] to correctly reduce to the known solutions for a spherical cap, $a/b = -1$, and for the circular plate, for which both a and $b \rightarrow \infty$.

Particular solutions

In addition to the solutions to the homogeneous equations, we now seek to obtain particular solutions to equation (1). A particular solution, expressed in polar coordinates, which will satisfy equation (1) for a uniformly distributed normal load q is:

$$\eta = \frac{-qar^2}{4} (1 - \cos 2\theta). \quad (15)$$

For the case of a uniform temperature, T , the right sides of equation (1) vanish identically and the effect of temperature is felt only through the expressions for strain in the constitutive equations, i.e. the additional strain due to temperature is expressed as:

$$\varepsilon_r = \varepsilon_\theta = \alpha T. \quad (16)$$

For the case of a temperature gradient across the shell, \bar{T}/t , equations (1) are again homogeneous and the influence of the temperature gradient is felt principally through an added term in the expression for the bending moment:

$$M_r = \frac{-K\bar{\alpha}\bar{T}(1+\nu)}{t}. \quad (17)$$

The three cases of distributed loading, for which equations (15)–(17) are particular solutions, are used to obtain solutions for the concentrated form of a similar loading, i.e. the concentrated normal force P , the concentrated thermal load μ (plane hot spot) and the concentrated thermal gradient $\bar{\mu}$ (bending hot spot).

Stress resultants and displacements

The solution η contains terms with both real and imaginary coefficients. The real and imaginary parts of the solution are associated with corresponding parts in the definitions of η , equations (3), to obtain real expressions for Φ and w . Solutions generated from (3a) will be written with constants A', \dots and those generated from (3b) with constants A'', \dots . The stress resultants are obtained by substituting in the appropriate relationships involving Φ and w :

$$\begin{aligned}
 N_r &= \frac{1}{r} \Phi_{,r} + \frac{1}{r^2} \Phi_{,\theta\theta} \\
 N_\theta &= \Phi_{,rr} \\
 N_{r\theta} &= \frac{1}{r^2} \Phi_{,\theta} - \frac{1}{r} \Phi_{,\theta r} \\
 M_r &= -K \left[w_{,rr} + \nu \left(\frac{w_{,r}}{r} + \frac{1}{r^2} w_{,\theta} \right) \right] \\
 M_{r\theta} &= -(1-\nu)K \left[\frac{1}{r} w_{,r\theta} - \frac{1}{r^2} w_{,\theta} \right] \\
 M_\theta &= -K \left[\frac{1}{r} w_{,r} + \frac{1}{r^2} w_{,\theta\theta} + \nu w_{,rr} \right] \\
 Q_r &= -K \left[w_{,rrr} + \frac{1}{r} w_{,rr} - \frac{1}{r^2} w_{,r} + \frac{1}{r^2} w_{,\theta\theta r} - \frac{2}{r^3} w_{,\theta\theta} \right] \\
 Q_\theta &= -K \left[\frac{1}{r} w_{,rr\theta} + \frac{1}{r^2} w_{,\theta r} + \frac{1}{r^3} w_{,\theta\theta\theta} \right].
 \end{aligned} \tag{18}$$

The positive direction of the stress resultants is shown in Fig. 4. The strains are obtained through the use of the constitutive relationships:

$$\begin{aligned}
 \varepsilon_r &= \frac{1}{Et} (N_r - \nu N_\theta) \\
 \varepsilon_\theta &= \frac{1}{Et} (N_\theta - \nu N_r) \\
 \gamma_{r\theta} &= \frac{2(1+\nu)}{Et} N_{r\theta}.
 \end{aligned} \tag{19}$$

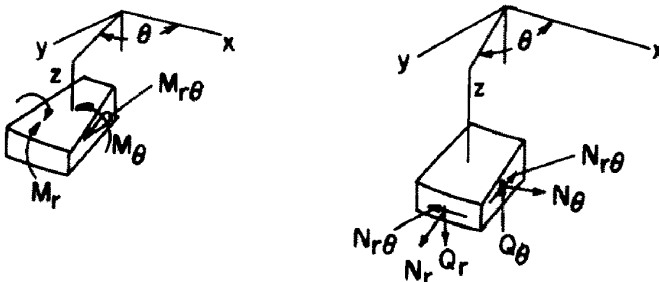


FIG. 4. Stress resultants acting on shell element.

Displacements are obtained by successive integration of the kinematic equations :

$$\begin{aligned} u_{,r} &= \varepsilon_r + w z_{,rr} \\ v_{,\theta} &= r\varepsilon_{\theta} - u + w \left(z_{,r} + \frac{z_{,\theta\theta}}{r} \right) \\ \gamma_{r\theta} &= v_{,r} + \frac{u_{,\theta}}{r} - \frac{v}{r} - 2w \left(\frac{z_{,\theta r}}{r} - \frac{z_{,\theta}}{r^2} \right). \end{aligned} \quad (20)$$

When the first two of equations (20) are integrated to produce u and v , arbitrary functions of integration are introduced ; the third of equations (20) is used to evaluate these functions. Although the expressions for displacement are cumbersome and are not shown here, the procedure used to obtain them is completely straightforward. In most instances, the arbitrary functions of integration are rigid-body displacements, which may be discarded ; in several instances, however, the arbitrary functions include discontinuous displacements, commonly called dislocations [7] and these are retained in the solution.

Convergence of solutions

The solutions such as expressed by equation (14) are written in terms of infinite series which have been assumed uniformly convergent during the initial stages of manipulating the governing differential equations. Since each term of the solution has an explicit expression, the proof of convergence of the solutions may be performed in a straightforward manner, by means of the "ratio test" [10] for the power series, and by means of the "Weierstrass comparison test" [10] for the harmonic series. Absolute and uniform convergence has been demonstrated [2] for both the regular and the singular solutions, for all values a/b , and for values of radius within the scope of shallow shell theory. The rate of convergence in each instance is at least as rapid as $1/n^2$.

IDENTIFICATION OF SINGULARITIES

The method used to identify the simpler singularities is to obtain the solution for a shell with distributed loading over a finite area, and then to reduce the area of loading while maintaining the load resultant constant. The result of this limiting process, as the loaded area approaches zero, is the desired singular solution associated with the applied load resultant. The term loading is here intended to denote both the application of force and of heat.

As a specific example, the concentrated force singularity is identified by first finding the solution for a shell having a uniformly distributed loading q over a specified region, $r < \rho$. This is illustrated in Fig. 5. The required solution is obtained by letting $\rho \rightarrow 0$ and $q \rightarrow \infty$ so that the load resultant, $\pi\rho^2q = P$, remains a constant.

In order to find the solution for the distributed loading, the shell is divided into two zones ; zone 1 has a uniformly distributed load and zone 2 is unloaded. A solution is then found for each of the shells individually. The arbitrary constants of the two sets of solutions are determined by fulfilling the boundary conditions at the outer boundary of zone 2, and by matching appropriate boundary conditions at the common boundary of the two zones, i.e. at $r = \rho$.

The stress resultants and displacements in both regions of the shell are required to be finite for the distributed loading. Therefore, the total solution in zone 1 consists of those

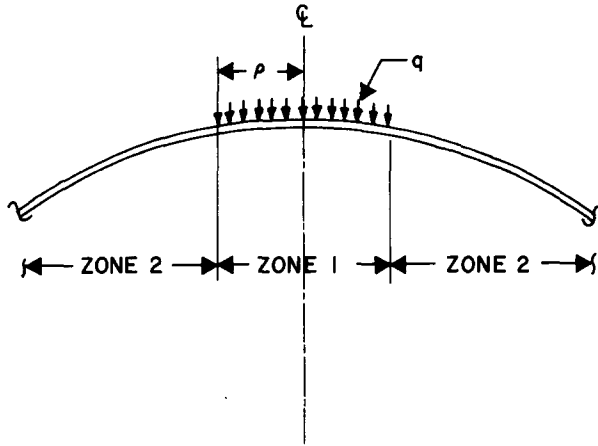


FIG. 5. Distributed loading applied to zone 1 of shell.

solutions to the homogeneous equation (4) which are free of singularities at the origin (constants A and B), plus a particular solution corresponding to the external load. In general, the solution for zone 2 consists of all solutions to the homogeneous differential equation. Certain simplifications are possible, however, if we restrict the solutions for zone 2 to the set of singular solutions (constants C and D), and leave the boundary conditions at the other boundary unspecified. Specific boundary conditions at this boundary can subsequently be fulfilled by the addition of regular solutions to the combined shell, zones 1 and 2. Since the regular solutions which we add do not have singularities at the origin, their influence will not be felt when we apply the limiting process, $\rho \rightarrow 0$.

The constants of the solution are determined by matching appropriate boundary conditions at the common boundary of the two zones of the shell. These are:

$$\begin{array}{ll}
 \text{(a) } w_1 = w_2 & \text{(e) } (N_r)_1 = (N_r)_2 \\
 \text{(b) } (w_r)_1 = (w_r)_2 & \text{(f) } (N_{r\theta})_1 = (N_{r\theta})_2 \\
 \text{(c) } (M_r)_1 = (M_r)_2 & \text{(g) } u_1 = u_2 \\
 \text{(d) } (Q_r)_1 = (Q_r)_2 & \text{(h) } v_1 = v_2.
 \end{array} \tag{21}$$

Subscripts 1 and 2 refer to the two zones of the shell. The boundary equations (21), when written out in detail, are rather cumbersome and will not be shown here. Each equation includes an infinite number of harmonics, and 8 times infinitely many constants. A direct solution for the constants in these equations is difficult. However, the boundary equations are made considerably simpler if we apply the limiting process, such that the area of loading approaches zero, prior to solving for the constants. This may legitimately be done as long as the determinant of the coefficients of the unknown constants remains non-singular, and the terms in the equations involving q , T and \bar{T} do not all vanish. When the limiting process is applied to the equations, it may be shown [2] that all constants, except for the first 7, approach zero as a limiting value. The first 7 constants are evaluated by solving surviving

portions of the first 7 equations:

$$\begin{aligned}
 \text{(a)} \quad & A_0'' + (B_0'\rho^2) - C_0'' \log \rho & & = 0 \\
 \text{(b)} \quad & 2(B_0'\rho^2) - C_0'' & & = 0 \\
 \text{(c)} \quad & -2(1+\nu)K(B_0'\rho^2) - K(1-\nu)C_0'' & & = \frac{K(1+\nu)\bar{\mu}}{\pi t} \\
 \text{(d)} \quad & 4KD_0' - \frac{\alpha}{a}(B_0''\rho^2) & & = \frac{P}{2\pi} \\
 \text{(e)} \quad & 2(B_0''\rho^2) - C_0' & & = 0 \\
 \text{(f)} \quad & \frac{2(1-\nu)}{Et}(B_0''\rho^2) + \frac{(1+\nu)}{Et}C_0' & & = -\frac{\mu}{\pi} \\
 \text{(g)} \quad & \frac{-\alpha}{2a}C_0'' & & -\frac{4D_0''}{Et} = 0.
 \end{aligned} \tag{22}$$

Equations (22) may be solved for the constants, in a straightforward manner, using each of the particular solutions individually. The results of interest are only those associated with the outer region 2, since the constants for region 1 describe the shell for only a vanishingly small region. The results for the constants of region 2 are:

1. Concentrated force

$$\begin{aligned}
 D_0' &= \frac{P}{8\pi K} \\
 C_0' &= C_0'' = D_0'' = 0.
 \end{aligned}$$

2. Plane hot spot

$$\begin{aligned}
 C_0' &= \frac{-\mu}{2\pi}Et \\
 D_0' &= \frac{-\mu\alpha Et}{16\pi Ka} \\
 C_0'' &= D_0'' = 0.
 \end{aligned}$$

3. Bending hot spot

$$\begin{aligned}
 C_0'' &= \frac{-(1+\nu)\bar{\mu}}{2\pi t} \\
 D_0'' &= \frac{\alpha(1+\nu)}{16\pi a}E\bar{\mu} \\
 C_0' &= D_0' = 0.
 \end{aligned}$$

The complete solution for the concentrated loading may now be determined from the appropriate values of Φ and w . The leading terms of the series for these quantities are:

1. Concentrated force

$$\Phi = -\frac{EtP(1-a/b)}{256\pi aK}[r^4 \log r + \dots]$$

$$w = \frac{P}{8\pi K}[r^2 \log r + \dots].$$

2. Plane hot spot

$$\Phi = -\frac{\mu Et}{2\pi}[\log r + \dots]$$

$$w = -\frac{\mu Et}{16\pi Ka} \left\{ \left[\left(1 - \frac{a}{b}\right) - \frac{1}{2} \left(1 + \frac{a}{b}\right) \cos 2\theta \right] r^2 \log r + \dots \right\}.$$

3. Bending hot spot

$$\Phi = \frac{(1+\nu)E\bar{\mu}(1-a/b)}{16\pi a}[r^2 \log r + \dots]$$

$$w = -\frac{(1+\nu)\bar{\mu}}{2\pi t}[\log r + \dots].$$

The complete solutions may be obtained by substituting the values of the appropriate constants in the solutions for η given by equation (14).

NUMERICAL RESULTS

To illustrate the use of the solutions such as given by equation (14), we have selected the case of the concentrated force acting on shells with variable a/b . The boundary conditions selected for the outer edge of the shell are those associated with a built in edge, i.e. $w = w_{,r} = u = v = 0$. Figure 6 illustrates the loading and edge support prevailing for the numerical examples.

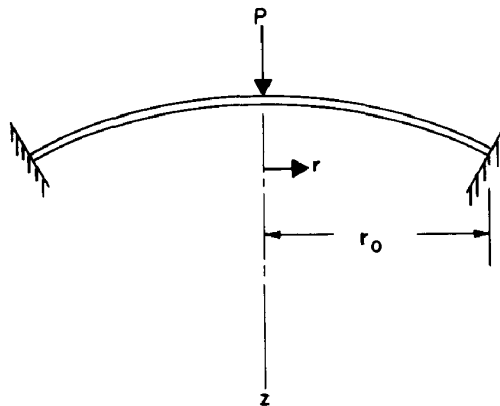


FIG. 6. Loading and support for shell with concentrated load.

In our previous discussion, we have shown that the only singular solution which has non zero value for the region outside of the area of loading is that associated with the constant D'_0 , which has value:

$$D'_0 = P/8\pi K.$$

In order to fulfill the specified boundary conditions at the edge of the shell, we now add all the regular solutions applicable to zone 2. When the boundary conditions are written in terms of all applicable solutions in zone 2, we obtain 4 separate equations for each harmonic: each of the equations contains a contribution from the singular solution, as well as contributions from each of the regular solutions headed by constants A'_p , A''_p , B'_p and B''_p , where $p = 0, 2, 4, \dots \infty$. Although the exact solution to the infinite set of equations may not be obtained readily, a good approximation to the solution can be made for most cases of interest by considering only finite segments of the set of equations. Thus, for the case of the concentrated load, we obtain an approximate solution by considering only the first 19 equations and the first 19 constants. This has been shown [2] to produce accurate results for all ratios a/b .

For the numerical example, we have chosen a dimensionless outer edge radius $cr_0 = 5$, and a value of Poisson's ratio $\nu = 0.3$. The power series for each harmonic, for both regular and singular solutions, were evaluated with the help of an electronic computer. The power series, which consist of terms with alternating signs, were truncated when succeeding terms progressively decreased in magnitude, and each additional term was $<10^{-6}$ times the accumulated sum. The solution of the simultaneous equations, and the final evaluation of w , w_r , and the stress resultants was also performed by the computer. The stress resultants and the displacement w , obtained for these calculations, are shown in Figs. 7-12. In Figs. 7-9, we have also shown the appropriate values for the flat, circular plate, as a basis for comparing similar curves for the shells. The solutions for the plate stem from the well known solution for the normal displacement [11]:

$$w = \frac{Pr_0^2}{16\pi K} \left[2 \left(\frac{r}{r_0} \right)^2 \log \left(\frac{r}{r_0} \right) + 1 - \left(\frac{r}{r_0} \right)^2 \right].$$

Although the circular plate does not completely fit the pattern of the shells being studied, it does represent a limiting case, and hence is used as a basis for comparison.

Figure 7, which presents the normal displacement w as a function of the radius ratio r/r_0 , for various values of a/b , demonstrates the effect of shell geometry on the overall stiffness, or the effective spring constant, of the various shells. The stiffness of all shells is seen to be considerably greater than that of the circular plate; of the shell forms studied, the sphere exhibits the greatest stiffness, while the cylinder exhibits the least stiffness. All shell forms exhibit negative displacements for the outer portion of the shell, in contrast to the plate which has everywhere a positive displacement for $r < r_0$.

Figure 8, which presents the bending moment M_r , as a function of radius ratio, indicates that the cylinder has the largest value of edge moment, while the sphere has the least value. The general pattern of distribution of moments is quite similar for all the shells, although considerably different from that of the plate. The bending moment M_r , for the shells as well as for the plate, approaches infinity as $r/r_0 \rightarrow 0$. However, the value of M_r reduces in value much more rapidly for the shells than it does for the plate, as r increases in value from the origin; hence, the effect of bending in the region surrounding the point of loading is con-

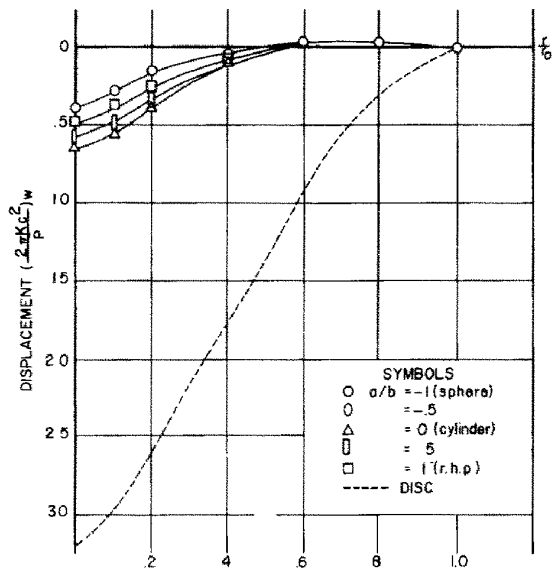


FIG. 7. Normal displacement w vs. r/r_0 , for concentrated force applied to shallow shells with variable a/b . Section taken through $\theta = 0$.

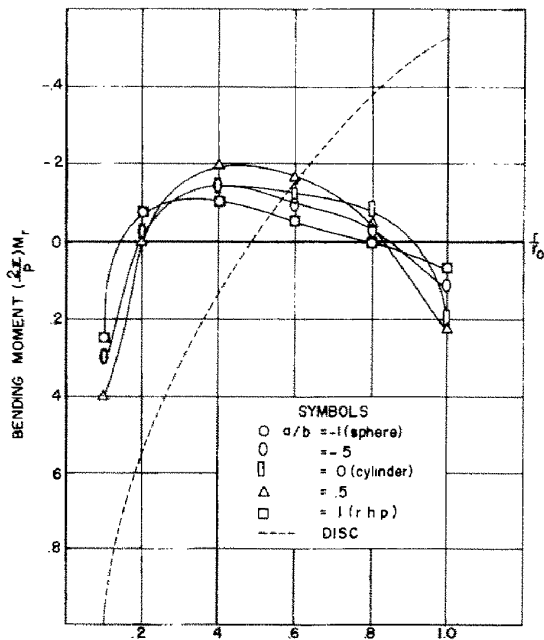


FIG. 8. Bending moment M_r vs. r/r_0 , for concentrated force applied to shallow shells with variable a/b . Section taken through $\theta = 0$.

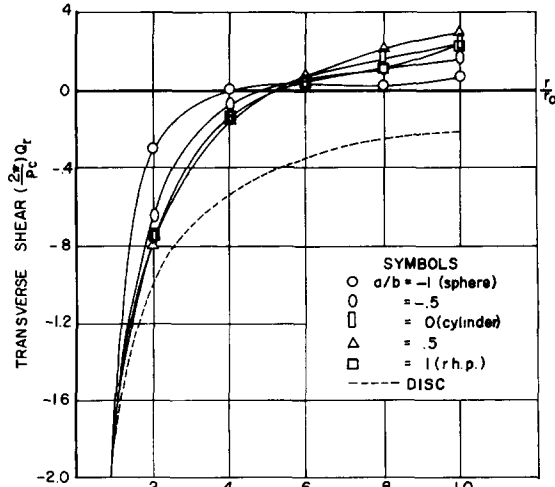


FIG. 9. Transverse shear Q_r vs. r/r_0 , for concentrated force applied to shallow shells with variable a/b . Section taken through $\theta = 0$.

siderably more localized for the case of the shells than it is for the plate. The distribution of Q_r , shown in Fig. 9, also indicates that the shells behave similar to the plate near the origin, but deviate in behavior rather rapidly as r/r_0 increases.

Figures 10–12 display the distribution of the in-plane stress resultants N_r , N_θ and $N_{r\theta}$. Although the in-plane force N_r , shown in Fig. 10, does not appear particularly sensitive to shell form, the distribution of N_θ , and $N_{r\theta}$, is significantly different for the various ratios a/b . At the origin, $r/r_0 = 0$, the shells of negative curvature exhibit larger shear forces $N_{r\theta}$, and smaller tangential forces N_r , than do shells of positive curvature. For the cylinder, the values of N_θ and $N_{r\theta}$ generally are intermediate in value between those for shells of positive curvature and those of negative curvature.

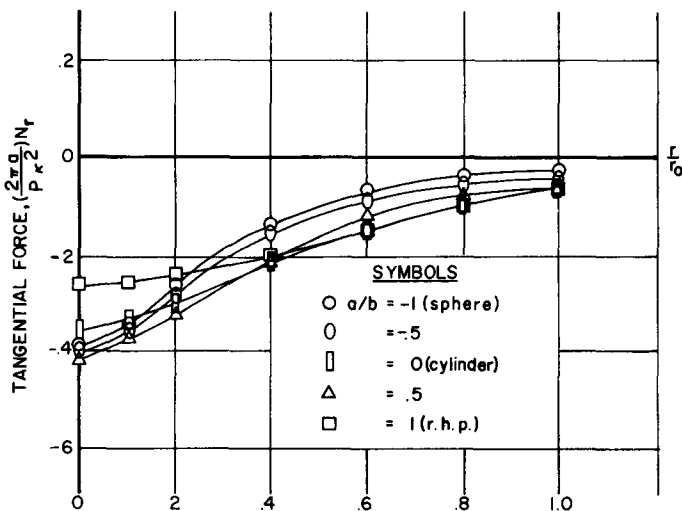


FIG. 10. Tangential force N_r vs. r/r_0 , for concentrated force applied to shallow shells with variable a/b . Section taken through $\theta = 0$.

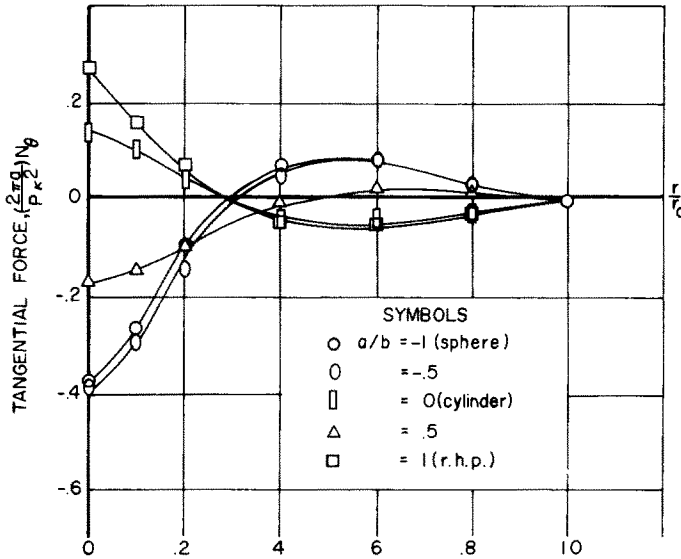


FIG. 11. Tangential force N_θ vs. r/r_0 , for concentrated force applied to shallow shells with variable a/b . Section taken through $\theta = 0$.

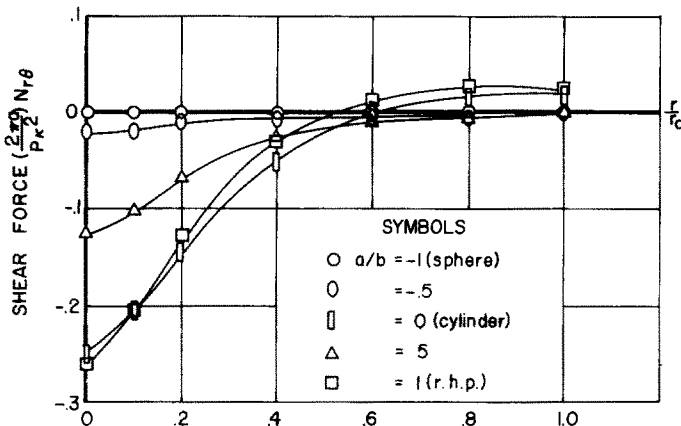


FIG. 12. Shear force $N_{r\theta}$ vs. r/r_0 , for concentrated force applied to shallow shells with variable a/b . Section taken through $\theta = 45^\circ$.

REFERENCES

- [1] G. N. CHERNYSHEV, On the action of concentrated forces and moments on an elastic thin shell of arbitrary shape. *J. appl. Math. Mech.* **27**, 172-184 (1963).
- [2] R. E. ELLING, Singular Solutions for Shallow Shells, Thesis presented to Stanford University in partial fulfillment of the requirements for the degree of Doctor of Philosophy (1967).
- [3] K. FORSBERG and W. FLÜGGE, Point load on a shallow elliptic paraboloid. *J. appl. Mech.* **33**, 575-585 (1966).
- [4] W. FLÜGGE, *Statik und Dynamik der Schalen*, 3rd edition, pp. 202-204, Springer (1962).
- [5] W. FLÜGGE and D. A. CONRAD, Thermal Singularities for Cylindrical Shells, *Proceedings, Third U.S. National Congress of Applied Mechanics*, pp. 321-328 (1958).

- [6] E. L. INCE, *Ordinary Differential Equations*, pp. 158–185. Dover (1956).
- [7] CH. MASSONNET, Two-dimensional Problems in Elasticity, *Handbook of Engineering Mechanics*, 1st edition, edited by W. FLÜGGE, pp. 1–3. McGraw-Hill (1962).
- [8] J. L. SANDERS and J. G. SIMMONDS, Concentrated force on shallow cylindrical shells. *J. appl. Mech.* **37**, 367–373 (1970).
- [9] J. L. SANDERS, Singular solutions to the shallow shell equations. *J. appl. Mech.* **37**, 361–364 (1970).
- [10] A. E. TAYLOR, *Advanced Calculus*, 1st edition, pp. 539–604. Blaisdell (1955).
- [11] S. TIMOSHENKO and S. WOINOWSKY-KRIEGER, *Theory of Plates and Shells*, 2nd edition, pp. 67–69, 285–289. McGraw-Hill (1959).
- [12] J. W. YOUNG, Singular Solutions for Non-Shallow Dome Shells, Thesis presented to Stanford University in Partial Fulfillment of the Requirements for the Degree of Doctor of Philosophy (1963).

(Received 27 October 1970; revised 4 August 1971)

Абстракт—Даются решения для неосрво-симметрической пологой оболочки, подверженной действию нормальной поверхностной или термической нагрузок. Отождествляются сингулярные решения, соответствующие сосредоточенной нормальной нагрузке сосредоточенному нагреву и сосредоточенному термическому градиенту, путем ограничения процесса, применяемого для полной системы сингулярных решений. Даются численные результаты, для случая нормальной, сосредоточенной нагрузки, действующей на полругую оболочку, обладающую отрицательной, нулевой или положительной кривизной Гаусса.

Поведение пологой оболочки, в соседстве приложенной сосредоточенной нагрузки, похоже к такому же поведению диска, подверженного той самой нагрузке.

Распространяется влияние сосредоточенной силы на всю широкую область оболочек с отрицательной кривизной Гаусса, по сравнению с оболочками с положительной кривизной Гаусса. Однако для случая сосредоточенной нагрузки, параметры напряжений и изгибов оболочки, не изменяются стремительно, если кривизна оболочки Гаусса изменяет значение из положительного к отрицательному.